Heliyon 10 (2024) e36386

Contents lists available at ScienceDirect

Heliyon

journal homepage: www.cell.com/heliyon

Research article

HL-60 cells as a valuable model to study LPS-induced neutrophil extracellular traps release

Sonya J. Malavez-Cajigas [a], Fabiana I. Marini-Martinez [a], Mercedes Lacourt-Ventura [a], Karla J. Rosario-Pacheco [a], Natalia M. Ortiz-Perez [a], Bethzaly Velazquez-Perez [a], Wilfredo De Jesús-Rojas [a], Daniel S. Chertow [b], Jeffrey R. Strich [b], Marcos J. Ramos-Benítez [a,*]

[a] *Ponce Health Sciences University & Ponce Research Institute, Ponce, Puerto Rico, 00716, USA*
[b] *Critical Care Medicine Department, National Institutes of Health Clinical Center, Bethesda, MD, 20814, USA*

ARTICLE INFO

Keywords:
Neutrophils
Neutrophil Extracellular Traps
Lipopolysaccharide
SYK inhibitor
Human leukemia cell line
HL-60

ABSTRACT

Neutrophil Extracellular Traps (NETs) present a paradoxical role in infectious diseases, contributing to both immunity and pathogenesis. The complex nature of this process necessitates further characterization to elucidate its clinical implications. However, studying NETs faces challenges with primary neutrophils due to their heterogeneity, short lifespan, and lack of adequate cryopreservation. Researchers often turn to alternative models, such as differentiated HL-60 cells (dHL-60). This study explored LPS-induced NETs formation in dHL-60 cells, revealing significant responses to LPS from *Pseudomonas aeruginosa*, although significantly lower than primary neutrophils. Moreover, Spleen Tyrosine Kinase (SYK) inhibition with R406, the active metabolite of the drug Fostamatinib, previously demonstrated to suppress NETs in primary neutrophils, effectively reduced NETs release in dHL-60 cells. dHL-60 cells, offering easier manipulation, consistent availability, and no donor variability in functional responses, possess characteristics suitable for high-throughput studies evaluating NETosis. Overall, dHL-60 cells may be a valuable in vitro model for deciphering the molecular mechanisms of NETosis in response to LPS, contributing to our available tools for understanding this complex immune process.

1. Introduction

Neutrophil Extracellular Traps (NETs), web-like structures composed of DNA, histones, and antimicrobial proteins, have emerged as key players in inflammation [1]. Interestingly, NETs are crucial in limiting pathogen spread and promoting microbial clearance, but excessive or uncontrolled formation can contribute to tissue damage and disease severity [2,3]. Therefore, a comprehensive understanding of NETs formation mechanisms is crucial for advancing our knowledge in this field. *In vitro* studies of NETs are directly influenced by the challenges associated with studying primary neutrophils. For example, their short lifespan restricts the duration of experiments, demanding precise timing for neutrophil isolation [4]. Moreover, their fragility and sensitivity require careful handling, their heterogeneity complicates data interpretation [5,6], and the lack of effective cryopreservation significantly impedes the effective planning of experiments and undermines overall feasibility [7]. In studies that aim to characterize molecular mechanisms, these

* Corresponding author.
E-mail address: mjramos@psm.edu (M.J. Ramos-Benítez).

https://doi.org/10.1016/j.heliyon.2024.e36386
Received 20 April 2024; Received in revised form 13 August 2024; Accepted 14 August 2024
Available online 20 August 2024

limitations of neutrophils can pose significant challenges. Thus, researchers have turned to alternative models such as HL-60 cells, a promyelocytic cell line derived from human leukemia, which can be differentiated into neutrophil-like cells (dHL-60) [7,8].

Utilizing dHL-60 cell lines, previous studies have made significant progress in describing neutrophil functional responses [9–12]. All-trans retinoic acid (ATRA), dimethylformamide (DMF) and dimethyl sulfoxide (DMSO) have been used as differentiation compounds to generate dHL-60 cells [8,9]. These studies agreed that NETs are generated in dHL-60 cells in response to Phorbol 12-myristate 13-acetate (PMA), a protein kinase C activator, under all three differentiation conditions. Manda-Handzlik et al. demonstrated that cells differentiated with DMF exhibited a response to calcium ionophore (CI) and PMA, whereas DMSO-differentiated cells only formed NETs in response to PMA [9]. This suggests that the differentiation conditions employed may impact the capacity of dHL-60 cells to form NETs in response to specific stimuli. Accordingly, it has been identified that DMSO-differentiated cells possess higher sensitivity to Toll like receptor 4 (TLR-4) ligands, such as lipopolysaccharide (LPS) [13].

While primary neutrophils have been observed to release NETs in response to LPS, a potent inflammatory stimulant from gram-

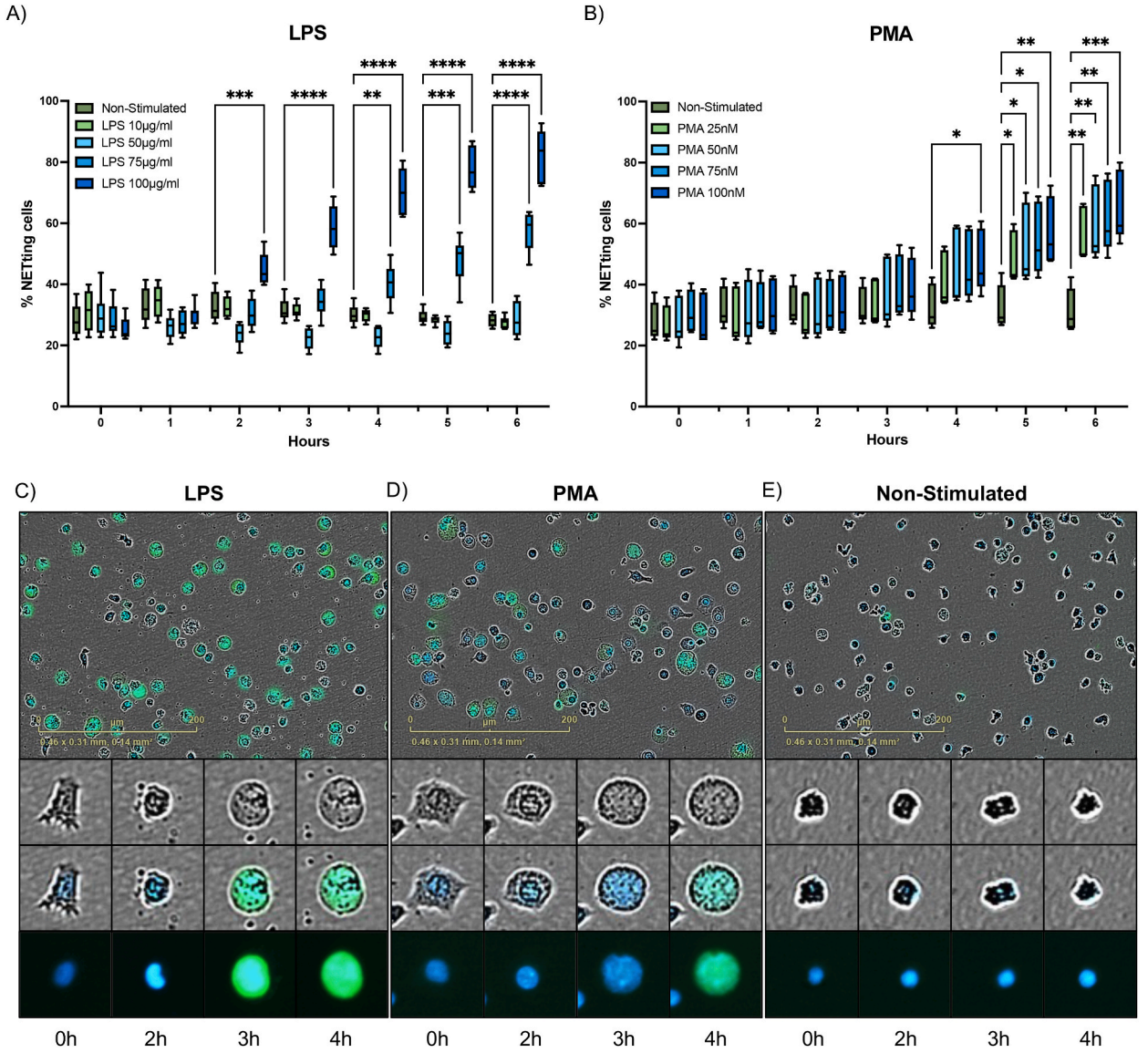

Fig. 1. LPS induces NETosis comparable to PMA in dHL-60 cells. The percent of dHL-60 cells undergoing NETosis ($n = 4$) after stimulation with A) Different concentrations of LPS from *P. aeruginosa* and B) Different concentrations of PMA, compared to non-stimulated dHL-60 cells. Representative images (20×) showing nuclei (blue fluorescence) and DNA release labeling (green fluorescence) at 6 h after stimulation with C) LPS (100 µg/mL), D) PMA (100 nM) or E) non-stimulated cells are shown. NETs are quantified by total fluorescence object area (µm^2/image) using Incucyte NETosis assay. Analysis was performed using two-way ANOVA with multiple comparisons to assess differences across concentrations versus non-stimulated cells. *, $P < 0.05$; **, $P < 0.01$; ***, $P < 0.001$; ****, $P < 0.0001$. Data are graphed as box and whisker plots showing the max and min values.

negative bacteria [14], there remains an important gap in our understanding regarding the behavior of dHL-60 cells under similar stimulations. Therefore, we sought to address this knowledge gap by evaluating whether LPS induces the formation of NETs in dHL-60 cells. Moreover, recent studies have provided compelling evidence demonstrating the efficacy of spleen tyrosine kinase (SYK) inhibitors to ameliorate NETs in various inflammatory diseases [15–18]. Notably, R406, the active metabolite of Fostamatinib, has effectively inhibited the formation of NETs induced by plasma from patients with COVID-19 and LPS in primary neutrophils [19,20]. Consequently, it is important to evaluate whether these inhibitors, which have demonstrated their effectiveness in primary neutrophils, can be successfully translated to dHL-60 cells to establish a reliable model for evaluating LPS-induced NETs formation.

Our study presents a targeted assessment of NETs formation in dHL-60 cells following differentiation with DMSO and evaluate the response to LPS stimulation and the potential of R406 to inhibit NETs in this context. Our report contributes to the growing body of literature on NETs, highlighting the potential utility of dHL-60 cells as an experimental model for studying underlying mechanisms of LPS-induced NETs.

2. Results

2.1. NETosis increases in response to LPS stimulation in dHL-60 cells

To examine NETs release, we performed live cell imaging to evaluate morphological changes, nuclear structure, and quantify the percent of cells undergoing NETosis. We investigated the effects of LPS derived from *P. aeruginosa* as potential stimulant of NETosis and PMA, a commonly used compound to induce NETs release in dHL-60 cells. Distinct responses of dHL-60 cells were elicited by the four tested LPS concentrations from *P. aeruginosa*. At 2 h, a statistically significant increase in NETs release was observed at 100 μg/mL stimulation with *P. aeruginosa* LPS ($P < 0.001$) (Fig. 1A), when compared to non-stimulated dHL-60 cells. Starting at 4 h, dHL-60

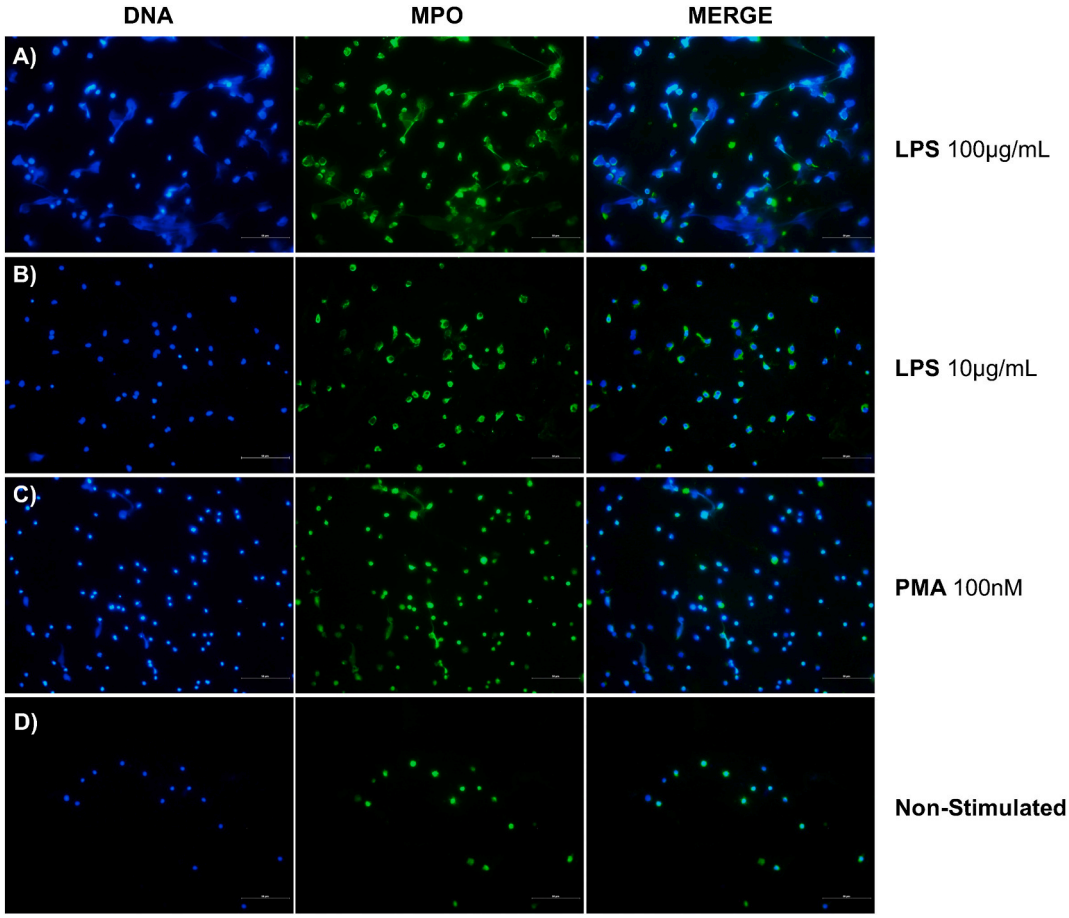

Fig. 2. Visualization of NETs MPO-DNA co-localization. Immunofluorescence staining was performed using antibodies targeting Myeloperoxidase (MPO), shown in green (FITC). DNA was counterstained with DAPI (4′,6-diamidino-2-phenylindole), shown in blue. This experiment was performed with dHL-60 cells stimulated with Lipopolysaccharide (LPS) from *P. aeruginosa* at A) 100 μg/mL and B) 10 μg/mL, C) PMA at 100 nM or D) non-stimulated. Cells were fixed after 2 h of stimulation. Representative images depict NETs structures with MPO-DNA co-localization. Images were captured at a magnification of 40×, and scale bar was set at 50 μm.

showed significantly higher NETosis levels when exposed to 100 μg/mL and 75 μg/mL of *P. aeruginosa* LPS ($P < 0.01$ and $P = 0.0001$ respectively) (Fig. 1A). In PMA stimulated dHL-60 cells, at 4 h a significant amount of NETosis was observed at 100 nM of PMA ($P < 0.05$) (Fig. 1B). By 5 h, all concentrations of PMA (25, 50, 75 and 100 nM) induced significant number of NETs, when compared to non-stimulated dHL-60 cells ($P < 0.05$) (Fig. 1B). NETosis was further confirmed and visualized using membrane permeable (blue) and nonpermeable (green) DNA labeling dyes. Representative images demonstrate similar changes leading to DNA release in 100 μg/mL of LPS and 100 nM of PMA stimulated groups at 6 h (Fig. 1C and D).

Like neutrophils, dHL-60 showed typical changes associated with NETosis in both stimulations (Fig. 1C and D). These changes include loss of nuclear lobulation, nuclear decondensation, integration of chromatin with cytoplasmic components, and eventual membrane breakdown, followed by staining with Cytotox green dye. Described changes were not observed in non-stimulated cells (Fig. 1E). It should be noted that cells may undergo NETosis at varying rates; therefore, the representative images we have provided summarize the overall process and its timing. However, it is possible to observe significant changes in cells at various time points.

To further confirm the process of NETosis, we performed a direct assessment using immunofluorescence staining. This involved the colocalization of DNA with myeloperoxidase (MPO). For this, we used earliest time point at which we detected signs of LPS-induced NETosis via live cell imaging as an endpoint (2 h). DNA web-like structures co-localizing with MPO were observed in cells stimulated with 100 μg/mL of *P. aeruginosa* LPS and 100 nM of PMA (Fig. 2B and D). Although notable morphological changes were observed, the DNA web-like structures were not present in 10 μg/mL of LPS (Fig. 2C). No morphological changes or NETs structures were observed in the non-stimulated cells (Fig. 2A). These results further corroborate the results shown in the live cells imaging analysis. We performed an MTT assay to confirm LPS- and PMA-induced effects were not influenced by immediate cytotoxicity. Following a 2-h incubation period, no differences were observed between cells stimulated with LPS or PMA and non-stimulated cells, indicating normal metabolic activity (Supplementary Fig. 1). This suggests that the cellular response was not triggered by mitochondrial dysfunction, which would typically occur in necrosis or advanced apoptosis stages.

Lastly, we aimed to understand how our findings in dHL-60 cells compared to the NETosis elicited by primary neutrophils after the LPS stimuli. For this, we stimulated primary neutrophils and dHL-60 cells side-by-side with 100 μg/mL of *P. aeruginosa* LPS which is the effective concentration for dHL-60. We found that the amount of NETosis was markedly different between the two cell types. By 6 h, primary neutrophils reached a 3000-fold change compared to 5-fold in dHL-60 cells when compared to their respective non-stimulated group (Supplementary Fig. 2).

2.2. R406 inhibits NETs formation in HL-60 cells

Previous studies have reported that R406, the active metabolite of Fostamatinib, effectively abrogates LPS-induced NETs in primary neutrophils [20]. Thus, we aimed to test its effectiveness in diminishing NETosis in response to LPS. For this, we pre-incubated dHL-60 cells with 1 μM of R406 for 30 min and stimulated with LPS. No differences were shown at 0- and 2-h post-stimulation. However, cells stimulated with LPS from *P. aeruginosa* exhibited significantly lower percentage of cells undergoing NETosis in the R406-treated group at 4- and 6-h post stimulation (Fig. 3), ($P < 0.05$). These findings suggest that dHL-60 cells can replicate the inhibitory effects of SYK inhibition on NETosis observed in primary neutrophils, further supporting the value of dHL-60 cells as a model for studying neutrophil responses to LPS.

3. Discussion

In this study, we demonstrate that stimulation with LPS alone from *P. aeruginosa* can induce NETs formation in dHL-60 cells, a process that can be inhibited with SYK inhibition using R406. We used LPS from a clinically relevant bacteria strain previously shown

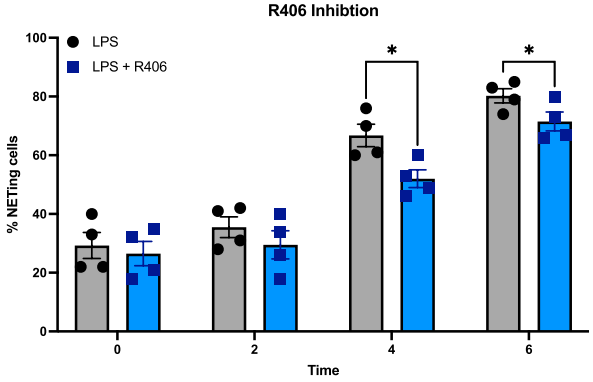

Fig. 3. R406 reduces LPS-induced NETosis in dHL-60 cells. NETs formation ($n = 4$) in dHL-60 cells after stimulation with LPS (100 μg/mL) *P. aeruginosa* alone or with a 30-min preincubation with R406. NETosis is showed as a percent of cells undergoing NETosis, per described in the methods section. NETs release is quantified by total green object area (μm^2/image) using Incucyte NETosis assay. Analysis was performed with multiple paired t-tests. *, $P < 0.05$; **, $P < 0.01$; ***, $P < 0.001$. Data are graphed in columns showing the mean ± SEM.

to induce NETs release in primary neutrophils [14,21]. The effective LPS concentration to induce NETosis in dHL-60 was 75 μg/mL and 100 μg/mL. These high concentrations have been previously reported in primarily neutrophils [22]. However, such concentrations are significantly higher than those typically used in LPS-induced NETs in primary neutrophils, which range from 10 ng/mL to 10 μg/mL [13,23–25]. Consistent with our data, a study by Neeli et al. showed that although histone citrullination is comparable in dHL-60 and primary neutrophils, dHL-60 require significantly higher concentrations of stimuli [26]. Various factors could influence these differences; first, HL-60-derived granulocytic cells have been reported to have low levels of TLR-4 expression, the sensing receptor for LPS in gram-negative bacteria [27]. However, a more recent study compared the effects of LPS on the expression levels of IL-1β and IL-8 in dHL-60 cells and PMN, revealing similar activation levels between both cell types. They conclude that the dHL-60 system can be effectively employed for studying TLR-4-mediated neutrophilic inflammatory responses [13]. Also, neutrophils have been described to perform NETs release in TLR-4-dependent and independent manner [14]. Thus, another possibility is that TLR-4 independent mechanisms predominate in dHL-60, thus requiring higher LPS concentrations to induce NETosis. These open questions support the need for further investigation to comprehensively study the mechanisms of LPS-induced NETosis in dHL-60 cells, including the role of TLR-4. Importantly, concentrations of 50 μg/mL or less did not induce NETosis, and a response was only observed at dosages above 75 μg/mL. This is consistent with previous studies documenting that LPS from *P. aeruginosa* must exceed a certain threshold concentration to induce NETosis, and lowering the concentration below this threshold does not yield a response curve [14].

To further evaluate the differences in effective concentration, we performed primary neutrophil stimulations at 100 μg/mL, the most effective concentration of LPS stimulation in dHL-60. Despite having similar trends and significant differences compared to their respective non-stimulated groups, the fold-change in NETs formation was markedly lower in dHL-60 cells than in primary neutrophils. Accordingly, other studies have shown that dHL-60 cells produced NETs, although to a much lower extent than primary neutrophils in response to PMA [28]. They suggest that a putative defect in the neutrophil NADPH oxidase enzyme complex could be a feasible explanation for the failure of dHL-60 cells to efficiently produce NETs in that context.

Even though high concentration of LPS were used, no cytotoxicity was evident as early metabolic activity was similar to non-stimulated cells. Live cell imaging allowed for the observation of NETosis related processes, induced by LPS and PMA, featuring nuclear decondensation, and subsequent cell membrane permeabilization, with DNA staining by non-permeable Cytotox green. These morphological changes we observed differed with those in other cell death mechanisms. For example, similar live cell imaging in primary neutrophils have shown apoptotic cells exhibit nuclear condensation and membrane blebbing, while necrotic cells experience rapid cell membrane disintegration with an intact nucleus [29]. Moreover, LPS has been shown to inhibit apoptosis in dHL-60 [30]. These distinctions and the immunofluorescence showing co-localization of DNA web structures and MPO, suggests that a NETosis pathway is being induced by the concentration of LPS used, distinct from apoptosis and necrosis.

In addition, we tested the role of the SYK signaling pathway using R406. This is particularly relevant as numerous cell surface receptors on neutrophils can induce functional responses via SYK signaling [31]. Previously, R406 effectively reduced NETosis in neutrophils stimulated with plasma from COVID-19 patients [19]. Also, SYK-PI3K-mTORC2 signaling pathway has been shown to mediate NETs release upon physiological stimuli exposure, such as opsonized *Staphylococcus aureus* [23]. Moreover, SYK inhibition with R406 abrogates neutrophil hyperactivation, including increased NETs formation, in response to LPS [20]. In our study, the effectiveness of R406 in significantly reducing NETosis induced by *P. aeruginosa* LPS was confirmed. Although statically significant, the inhibition by R406 was not as robust as shown in reports in primary neutrophils [20]. This may be due to two reasons: (1) a SYK-independent pathway may be operational in dHL-60 cells, and (2) there are higher levels of phosphorylated SYK in dHL-60 cells. It has been documented that the differentiation of HL-60 cells into neutrophil-like cells induces increased SYK activity, which may contribute to the reduced sensitivity to the inhibitor [32]. Yet, the data suggests that dHL-60 could serve as a valuable model to investigate the underlying mechanisms by which SYK inhibition leads to decreased NETs release, especially in contexts where genetic manipulation is required for mechanistic evaluations.

This study has several limitations. First, we aimed to test the use of dHL-60 cells as a model to replicate findings reported in primary neutrophils regarding LPS-induced NETs formation [20], and how SYK inhibition could reduce NETosis in these cells. Thus, this study lacks a detailed evaluation of underlying mechanisms. Second, while dHL-60 cells may serve as a valuable in vitro model for studying NETs in response to LPS, particularly in settings where the use of primary neutrophils poses significant limitations, they do not fully replicate the response of primary neutrophils, which could limit the physiological relevance of our findings. Additionally, their diminished response to LPS necessitates cautious interpretation when extrapolating these findings to *in vivo* settings. However, the study provides important insights into NETs formation in response to LPS stimulation using dHL-60 cells and highlights the potential utility of this model for further investigations, particularly those aiming to perform genetic modifications and detailed mechanistic studies on NETosis and the inhibitory role of R406.

4. Materials and methods

4.1. HL-60 cell culture and differentiation

The promyelocytic leukemia cell line HL-60 (American Type Culture Collection (ATCC), Manassas, Virginia, USA, Catalog No. CCL-240) was cultured in Iscove's Modified Dulbecco's Medium (IMDM) supplemented with 20 % non-heat inactivated fetal bovine serum (FBS), as indicated by ATCC and a previous study [33]. Cells were maintained in a humidified incubator at 37 °C with 5 % CO_2. For the differentiation process, we transferred cells into a new flask at a density of 1×10^6 cells/mL and incubated for 4 days (37 °C, 5 % CO_2) in IMDM supplemented with 10 % FBS, and 1.25 % DMSO. Note that for cell differentiation, the FBS concentration was reduced to 10 % following initial experiments that demonstrated enhanced NETs formation under these conditions (data not shown). Cell confluency

and differentiation status were assessed by morphological changes using a light microscope.

4.2. Primary neutrophils isolation

Neutrophils were isolated from blood collected from a single healthy donor. Following written informed consent, blood was drawn into an EDTA tube. The neutrophils were then isolated using the EasySep Direct Human Neutrophil Isolation Kit (STEMCELL Technologies), in accordance with the manufacturer's instructions. The sample collection was conducted under protocol number #2303138796A001, approved by the Ponce Research Institute Institutional Review Board on May 23, 2023.

4.3. Stimulation with lipopolysaccharide or Phorbol 12-myristate 13-acetate (PMA)

To induce NETs formation, dHL-60 cells or primary neutrophils were stimulated with LPS derived from *P. aeruginosa* (Sigma-Aldrich, Inc., St. Louis, Missouri, USA, Catalog No. L9143-25 MG) or PMA (Thermo Fisher Scientific, Waltham, Massachusetts, USA, Catalog No J63916-MNF-J3-06). To evaluate the possible dose-dependent effects on biological responses, we tested various concentrations of LPS (10, 50, 75, or 100 μg/mL) and PMA (25, 50, 75 or 100 nM), prepared in serum-free IMDM. Control groups we treated with serum-free IMDM only. After stimulation, the 96-well plate was placed in the Incucyte SX5 instrument for imaging acquisition.

4.4. NETs release live imaging and quantification

After protocol optimization, cells were seeded at 30,000 cells/well in a 100 μL. The Incucyte SX5 instrument (Sartorius AG, Göttingen, Germany) was set to acquire phase contrast and fluorescence images were captured using a 20× magnification. For fluorescence, exposure time was 300 ms for green and 150 ms for NIR. Four images per well were taken every 30 min from distinct regions of the well. The phase-contrast images and fluorescence using the Incucyte® Nuclight Rapid NIR (Essen BioScience Inc., Ann Arbor, Michigan, USA, Catalog No. 4804) allowed visualization on cell morphology, and nuclear decondensation, while the enhancement of green fluorescence using 250 nM of Cytotox Green (Essen BioScience Inc., Ann Arbor, Michigan, USA, Catalog No. 4633) permitted the visualization of DNA release. After acquisition, the software was trained to distinguish normal cells versus cells undergoing NETosis. Briefly, we provide the software with representative images from various time points of unstimulated cells and cells stimulated with the positive control (e.g., PMA). For these experiments, we applied the surface fit background correction with a set fluorescence threshold of 2 Green Calibrated Units (GCU), an edge sensitivity of −50 and a minimum area of 40 μm^2. For phase, classic confluence was used with a segmentation adjustment of 0.2, a minimum area filter of 50 μm^2 and a maximum eccentricity filter of 0.99. Using these parameters, the instrument's software automatically analyzed all the acquired images and calculated the cells counts and green fluorescence count (NETs), which was used to calculate percent of NETting cells (Green count/Cell count * 100). The percent of NETting cells was then used for comparison across experimental groups.

4.5. NETs immunofluorescence

Cells were seeded at a density of 100,000 cells/chamber in a 100 μL using a chambered slide (Ibidi USA Inc., WI, Catalog No. 80841) and treated as previously described. Cells were incubated for 2 h. Following incubation, the treatment was removed, and the cells were washed with PBS 1X. Cells were fixed using 4 % paraformaldehyde for 10 min, permeabilized with PBS 1X/0.01 % Triton X for 3 min, then blocked using UltraCruz® Blocking Reagent (Santa Cruz Biotechnology, CA, Catalog No. sc-516214) for 30 min. The staining was performed as described by Im K et al. [34]. The primary antibody Myeloperoxidase (Thermo Fisher Scientific, Waltham, Massachusetts, USA, Catalog No. r PA5-16672) was used at a dilution of 1:100 and incubated at RT for 1 h. Then the secondary antibody conjugated with FITC (Abcam Inc., MA, Catalog No. ab6717) was utilized at a dilution of 1:1000 (2 μg/mL) and incubated for 1 h at room temperature. DNA was counterstained with DAPI (Sigma-Aldrich, Inc., MO, Catalog No. D9542). Images were obtained with the BX60 Olympus microscope (Olympus Corp of Americas, PA) and analyzed with NIS-Elements AR 3.22.15 software (Nikon Instruments Inc., NY). Images were taken at 40× magnification and scale bar was set at 50 μm.

4.6. SYK inhibition

To test its effectiveness in dHL-60 cells, the SYK inhibitor R406 (Invivogen, Inc., San Diego, California, USA, Catalog No. inh-r406n) was tested at 1 μM prepared in IMDM. Cells were preincubated for 30 min with the inhibitor in a humidified incubator at 37 °C with 5 % CO_2. Live cells imaging and analysis was performed as described above.

4.7. MTT assay

Cells were seeded at a concentration of 250,000 cells/well in a 100 μL, stimulated with LPS, PMA, or non-stimulated as previously described, and incubated for 2 h. The assay was performed in accordance with manufacturer instructions (Sigma-Aldrich, Inc., MO, Catalog No. TOX-1). The MTT reagent was diluted in PBS 1X and incubated for 2 h. The absorbance was measured at 590 nm using a Synergy HT spectrophotometer (Agilent Technologies (Biotek), PA).

4.8. Statistical analysis

All statistical analyses were performed using GraphPad Prism version 10.2.0 for IOS, GraphPad Software, San Diego, CA, USA, www.graphpad.com. NETosis results are shown as a percent of number of cells undergoing NETosis or a fold change from non-stimulated cells. Paired T-test, one-way ANOVA or two-way ANOVA were used to test significance. Results were considered significant if $P < 0.05$.

Data availability statement

All relevant data supporting the findings of this study are included within the article, its supplementary materials, or are referenced therein. Additional data can be provided by the corresponding author upon request.

CRediT authorship contribution statement

Sonya J. Malavez-Cajigas: Writing – review & editing, Writing – original draft, Visualization, Methodology, Investigation, Formal analysis, Data curation, Conceptualization. **Fabiana I. Marini-Martinez:** Writing – review & editing, Writing – original draft, Visualization, Formal analysis. **Mercedes Lacourt-Ventura:** Writing – review & editing, Visualization, Supervision, Project administration, Methodology, Investigation, Funding acquisition. **Karla J. Rosario-Pacheco:** Writing – review & editing, Methodology, Investigation. **Natalia M. Ortiz-Perez:** Writing – review & editing, Methodology, Investigation. **Bethzaly Velazquez-Perez:** Writing – review & editing, Investigation. **Wilfredo De Jesús-Rojas:** Writing – review & editing, Visualization, Resources, Conceptualization. **Daniel S. Chertow:** Writing – review & editing, Visualization, Conceptualization. **Jeffrey R. Strich:** Writing – review & editing, Visualization, Conceptualization. **Marcos J. Ramos-Benítez:** Writing – review & editing, Visualization, Supervision, Resources, Project administration, Methodology, Investigation, Funding acquisition, Formal analysis, Data curation, Conceptualization.

Declaration of generative AI and AI-assisted technologies in the writing process

During the preparation of this work, the author(s) used ChatGPT to assist in editing the text for enhanced grammar and clarity. After using this tool/service, the author(s) reviewed and edited the content as needed and take(s) full responsibility for the content of the publication.

Declaration of competing interest

The authors declare that they have no known competing financial interests or personal relationships that could have appeared to influence the work reported in this paper.

Acknowledgements

This research was funded by Research Centers in Minority Institutions (RCMI) Center for Research Resources Grant and the Molecular and Genomics Core #U54MD007579. Hispanic Clinical and Translational Research Education and Career Development (HCTRECD) program #5R25MD007607-22, The Hispanic Alliance for Clinical and Translational Research - Mentor Mentee Program Grant #5U54GM133807-03 and PR-INBRE Developmental Research Project Program (DRPP) #5P20GM103475-21.

Appendix A. Supplementary data

Supplementary data to this article can be found online at https://doi.org/10.1016/j.heliyon.2024.e36386.

References

[1] V. Delgado-Rizo, et al., Neutrophil extracellular traps and its implications in inflammation: an overview, Front. Immunol. 8 (2017).
[2] A. Hidalgo, et al., Neutrophil extracellular traps: from physiology to pathology, Cardiovasc. Res. 118 (13) (2022) 2737–2753.
[3] V. Papayannopoulos, Neutrophil extracellular traps in immunity and disease, Nat. Rev. Immunol. 18 (2) (2018) 134–147.
[4] M. Stoimenou, et al., Methods for the assessment of NET formation: from neutrophil biology to translational research, Int. J. Mol. Sci. 23 (24) (2022).
[5] C. Silvestre-Roig, A. Hidalgo, O. Soehnlein, Neutrophil heterogeneity: implications for homeostasis and pathogenesis, Blood 127 (18) (2016) 2173–2181.
[6] L.G. Ng, R. Ostuni, A. Hidalgo, Heterogeneity of neutrophils, Nat. Rev. Immunol. 19 (4) (2019) 255–265.
[7] M. Blanter, M. Gouwy, S. Struyf, Studying neutrophil function in vitro: cell models and environmental factors, J. Inflamm. Res. 14 (2021) 141–162.
[8] Y. Guo, et al., Differentiation of HL-60 cells in serum-free hematopoietic cell media enhances the production of neutrophil extracellular traps, Exp. Ther. Med. 21 (4) (2021) 353.
[9] A. Manda-Handzlik, et al., The influence of agents differentiating HL-60 cells toward granulocyte-like cells on their ability to release neutrophil extracellular traps, Immunol. Cell Biol. 96 (4) (2018) 413–425.
[10] J. Zhao, et al., NETs promote inflammatory injury by activating cGAS-STING pathway in acute lung injury, Int. J. Mol. Sci. 24 (6) (2023) 5125.
[11] M. Sano, et al., Neutrophil extracellular traps-mediated Beclin-1 suppression aggravates atherosclerosis by inhibiting macrophage autophagy, Front. Cell Dev. Biol. 10 (2022).

[12] Y.-T. Hsieh, et al., Down-regulated miR-146a expression with increased neutrophil extracellular traps and apoptosis formation in autoimmune-mediated diffuse alveolar hemorrhage, J. Biomed. Sci. 29 (1) (2022) 62.
[13] T. Shuto, et al., Increased responsiveness to TLR2 and TLR4 ligands during dimethylsulfoxide-induced neutrophil-like differentiation of HL-60 myeloid leukemia cells, Leuk. Res. 31 (12) (2007) 1721–1728.
[14] E. Pieterse, et al., Neutrophils discriminate between lipopolysaccharides of different bacterial sources and selectively release neutrophil extracellular traps, Front. Immunol. 7 (2016) 484.
[15] N. Cooper, et al., Recent advances in understanding spleen tyrosine kinase (SYK) in human biology and disease, with a focus on fostamatinib, Platelets 34 (1) (2023) 2131751.
[16] S.a. Tang, Q. Yu, C. Ding, Investigational spleen tyrosine kinase (SYK) inhibitors for the treatment of autoimmune diseases, Expet Opin. Invest. Drugs 31 (3) (2022) 291–303.
[17] G. Wigerblad, et al., Spleen tyrosine kinase inhibition restores myeloid homeostasis in COVID-19, Sci. Adv. 9 (1) (2023) eade8272.
[18] J.R. Strich, et al., Fostamatinib for the treatment of hospitalized adults with coronavirus disease 2019: a randomized trial, Clin. Infect. Dis. 75 (1) (2021) e491–e498.
[19] J.R. Strich, et al., Fostamatinib inhibits neutrophils extracellular traps induced by COVID-19 patient plasma: a potential therapeutic, J. Infect. Dis. 223 (6) (2021) 981–984.
[20] S. Warner, et al., R406 reduces lipopolysaccharide-induced neutrophil activation, Cell. Immunol. 403–404 (2024) 104860.
[21] M.J. Kaplan, M. Radic, Neutrophil extracellular traps: double-edged swords of innate immunity, J. Immunol. 189 (6) (2012) 2689–2695.
[22] M. Sabbatini, et al., Aging hampers neutrophil extracellular traps (NETs) efficacy, Aging Clin. Exp. Res. 34 (10) (2022) 2345–2353.
[23] M. van der Linden, et al., Differential signalling and kinetics of neutrophil extracellular trap release revealed by quantitative live imaging, Sci. Rep. 7 (1) (2017) 6529.
[24] R. Arroyo, et al., SP-D attenuates LPS-induced formation of human neutrophil extracellular traps (NETs), protecting pulmonary surfactant inactivation by NETs, Commun. Biol. 2 (2019) 470.
[25] A. Petretto, et al., Neutrophil extracellular traps (NET) induced by different stimuli: a comparative proteomic analysis, PLoS One 14 (7) (2019) e0218946.
[26] I. Neeli, S.N. Khan, M. Radic, Histone deimination as a response to inflammatory stimuli in neutrophils, J. Immunol. 180 (3) (2008) 1895–1902.
[27] Y. Mita, et al., Induction of Toll-like receptor 4 in granulocytic and monocytic cells differentiated from HL-60 cells, Br. J. Haematol. 112 (4) (2001) 1041–1047.
[28] R. Yaseen, et al., Antimicrobial activity of HL-60 cells compared to primary blood-derived neutrophils against Staphylococcus aureus, J. Negat. Results Biomed. 16 (1) (2017) 2.
[29] S. Gupta, et al., A high-throughput real-time imaging technique to quantify NETosis and distinguish mechanisms of cell death in human neutrophils, J. Immunol. 200 (2) (2018) 869–879.
[30] J.C. Marshall, et al., Interleukin-1beta mediates LPS-induced inhibition of apoptosis in retinoic acid-differentiated HL-60 cells, Biochem. Biophys. Res. Commun. 369 (2) (2008) 532–538.
[31] K. Futosi, A. Mócsai, Tyrosine kinase signaling pathways in neutrophils, Immunol. Rev. 273 (1) (2016) 121–139.
[32] S. Qin, H. Yamamura, Up-regulation of syk activity during HL60 cell differentiation into granulocyte but not into monocyte/macrophage-lineage, Biochem. Biophys. Res. Commun. 236 (3) (1997) 697–701.
[33] J. Basu, et al., Molecular and epigenetic alterations in normal and malignant myelopoiesis in human leukemia 60 (HL60) promyelocytic cell line model, Front. Cell Dev. Biol. 11 (2023) 1060537.
[34] K. Im, et al., An introduction to performing immunofluorescence staining, Methods Mol. Biol. 1897 (2019) 299–311.